ACS APPLIED MATERIALS & INTERFACES

Research Article

www.acsami.org

Solution-Processed Small Molecules As Mixed Host for Highly Efficient Blue and White Phosphorescent Organic Light-Emitting Diodes

Qiang Fu, Jiangshan Chen,* Changsheng Shi, and Dongge Ma*

State Key Laboratory of Polymer Physics and Chemistry, Changchun Institute of Applied Chemistry, Chinese Academy of Sciences, Graduate School of Chinese Academy of Sciences, Changchun 130022, People's Republic of China

ABSTRACT: The widely used hole-transporting host 4,4′,4″-tris(N-carbazolyl)-triphenylamine (TCTA) blended with either a hole-transporting or an electron-transporting small-molecule material as a mixed-host was investigated in the phosphorescent organic light-emitting diodes (OLEDs) fabricated by the low-cost solution-process. The performance of the solution-processed OLEDs was found to be very sensitive to the composition of the mixed-host systems. The incorporation of the hole-transporting 1,1-bis[(di-4-tolylamino)phenyl]cyclohexane (TAPC) into TCTA as the mixed-host was demonstrated to greatly reduce the driving voltage and thus enhance the efficiency due to the improvement of hole injection and transport. On the basis of the mixed-host of TCTA:TAPC, we successfully fabricated low driving voltage and high efficiency blue and white phosphorescent OLEDs. A maximum forward viewing current efficiency of 32.0 cd/A and power efficiency of 25.9 lm/W were obtained in the optimized mixed-host blue OLED, which remained at 29.6 cd/A and 19.1 lm/W at the luminance of 1000 cd/m^2 with a driving voltage as low as 4.9 V. The maximum efficiencies of 37.1 cd/A and 32.1 lm/W were achieved in a single emissive layer white OLED based on the TCTA:TAPC mixed-host. Even at 1000 cd/m^2, the efficiencies still reach 34.2 cd/A and 23.3 lm/W and the driving voltage is only 4.6 V, which is comparable to those reported from the state-of-the-art vacuum-evaporation deposited white OLEDs.

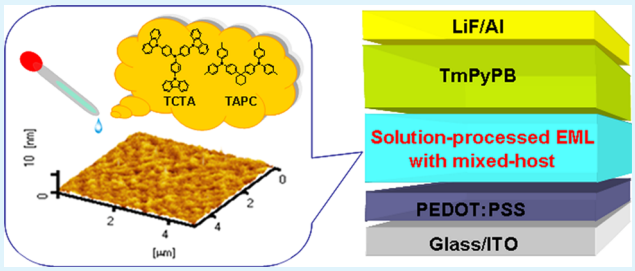

KEYWORDS: *solution-processed, small molecules, mixed-host, phosphorescence, blue and white OLEDs*

INTRODUCTION

Organic light-emitting diodes (OLEDs) have drawn considerable attention during the past decades because of their potential applications in flat-panel displays, solid-state lighting, and back-lighting sources for liquid-crystal displays.[1−5] Generally, OLEDs can be divided into two classes: the small molecule devices prepared by vacuum-evaporation deposition and polymer devices by solution-processing. So far the performances of the solution-processed polymer devices are inferior to those of the small molecule devices. Especially, the efficiencies of blue and white phosphorescent OLEDs based on polymers are still unsatisfactory because of lack of a polymeric host with high triplet energy for blue phosphors. Some small molecules were combined into polymer matrix to improve the device performance.[6−11] Although the current efficiencies of the OLEDs based on phosphor bis[(4,6-difluorophenyl)-pyridinato-N,C2](picolinate) iridium(III) (FIrpic) and polymers are achieved at a high level, the power efficiencies of the solution-processed blue and white phosphorescent OLEDs remain to be further improved to reduce energy consumption at high luminance.[12−14] Moreover, compared to the vacuum-evaporation deposition, the solution process is more feasible for the fabrication of the low-cost OLEDs because of its greater ease of processing and large-area manufacturability.[6,7] To achieve low-cost and high-performance, an effective strategy is to fabricate small molecule OLEDs by solution-process, which can combine the advantages of the low-cost solution process and the high performance of small molecule devices.

To achieve high-performance OLEDs by solution-processing, the formation of uniform amorphous films is a very important prerequisite, which strongly depends on the solution-processability of the used materials. Although a large number of small molecules have been developed for the OLEDs fabricated by vacuum-evaporation deposition, most of them are not suitable for solution processing because of factors such as inadequate solubility and crystallization tendency. Therefore, the development of small molecule materials with good solution-processability is very helpful for the high-performance, solution-processed, small-molecule OLEDs.[6,7,15−21]

In addition to the solution-processability of the small molecule materials, efficient charge injection and charge transport balance are also very important for the performance of solution-processed, small-molecule OLEDs. For these purposes, a widely used approach is to construct multilayered devices including charge injection and transport layers. However, it is difficult to form multilayered small-molecule films by solution process

Received: August 18, 2012
Accepted: November 9, 2012
Published: November 9, 2012

 © 2012 American Chemical Society

because the former film will be destroyed by subsequent processing. Although many efforts have been made to develop multilayered OLEDs by solution process, the driving voltages of these OLEDs are still too high to obtain high power efficiency.[16−19,22−25] Recently, an effective method of host engineering was proposed to improve the performance of solution-processed phosphorescent OLEDs. Mixed hosts, usually consisting of the hole- and electron-transporting materials, were employed to improve the charge balance and broaden the recombination zone in the solution-processed OLEDs.[9,16] More importantly, the mixed-host systems are beneficial to decrease crystallization, which is favored to improve the performance of the solution-processed OLEDs. In the mixed-host OLEDs, the solution-processed emissive layers (EML) were usually combined with a simply vacuum-evaporated electron-transporting/hole-blocking layer to avoid the quenching of excitons at the metal electrode interface. On the basis of this concept, a number of high-performance, solution-processed, small-molecule OLEDs were reported.[26−30] However, these solution-processed OLEDs, especially the blue phosphorescent OLEDs, have low power efficiency at an illumination-relevant luminance of 1000 cd/m^2. Hence, the further improvement of the balanced charge injection and transport is necessary to achieve low power efficiency roll-off in the solution-processed mixed-host OLEDs.

In this paper, high efficiency blue and white phosphorescent OLEDs were fabricated by solution-processing commercial small molecules as the mixed-hosts. The commonly used hole-transporting host 4,4′,4″-tris(N-carbazolyl)-triphenylamine (TCTA) doped with either the hole-transporting 1,1-bis[(di-4-tolylamino)phenyl]cyclohexane (TAPC) or the electron-transporting 1,3-bis[(4-tert-butylphenyl)-1,3,4,-oxadiazolyl]-phenylene (OXD-7) as the solution-processed mixed-host was investigated. It was found that the performance of the solution-processed blue OLEDs based on the phosphor bis[(4,6-difluorophenyl)-pyridinato-N,C2](picolinate) iridium-(III) (FIrpic) are very sensitive to the composition of the mixed-host systems. Doping TAPC into TCTA with moderate concentration can reduce the driving voltage and improve the efficiency in the blue OLEDs, on the contrary, doping OXD-7 into TCTA leads to the decreased efficiency. The maximum current and power efficiencies of 32.0 cd/A and 25.9 lm/W, respectively, were achieved in the optimized solution-processed blue OLED using TCTA:TAPC as the mixed-host, and remained at 29.6 cd/A and 19.1 lm/W at the luminance of 1000 cd/m^2. Based on the TCTA:TAPC mixed-host, highly efficient white OLEDs were also fabricated, the maximum efficiencies of 37.1 cd/A and 32.1 lm/W were achieved. Even at 1000 cd/m^2, the efficiencies still reach 34.2 cd/A and 23.3 lm/W.

EXPERIMENTAL SECTION

Materials. The hole-injection material of poly (styrene sulfonic acid)-doped poly (3, 4-ethylenedioxythiophene) (PEDOT:PSS, Baytron PVP AI4083) was purchased from H.C. Starck GmbH. The hole-transporting materials of 4,4′,4″-tris(N-carbazolyl)-triphenylamine (TCTA) and 1,1-bis[(di-4-tolylamino)phenyl] cyclohexane (TAPC), the electron-transporting materials of 1,3-bis[(4-tert-butylphenyl)-1,3,4,-oxadiazolyl]phenylene (OXD-7) and 1,3,5-tri(m-pyrid-3-yl-phenyl)-benzene (TmPyPB), and the phosphorescent dopants of bis[(4,6-difluorophenyl)-pyridinato-N,C^2](picolinate) iridium(III) (FIrpic), tris(2-phenylpyridine) iridium(III) (Ir(ppy)$_3$), and bis(2-methyldibenzo-[f,h]quinoxaline)(acetylacetonate) iridium(III) (Ir(MDQ)$_2$(acac)) were purchased from Nichem Fine Technology Co. Ltd. LiF and MoO_3 were purchased from Sigma-Aldrich. All materials were used as received. The chemical structures of the used small molecule materials are shown in Figure 1a.

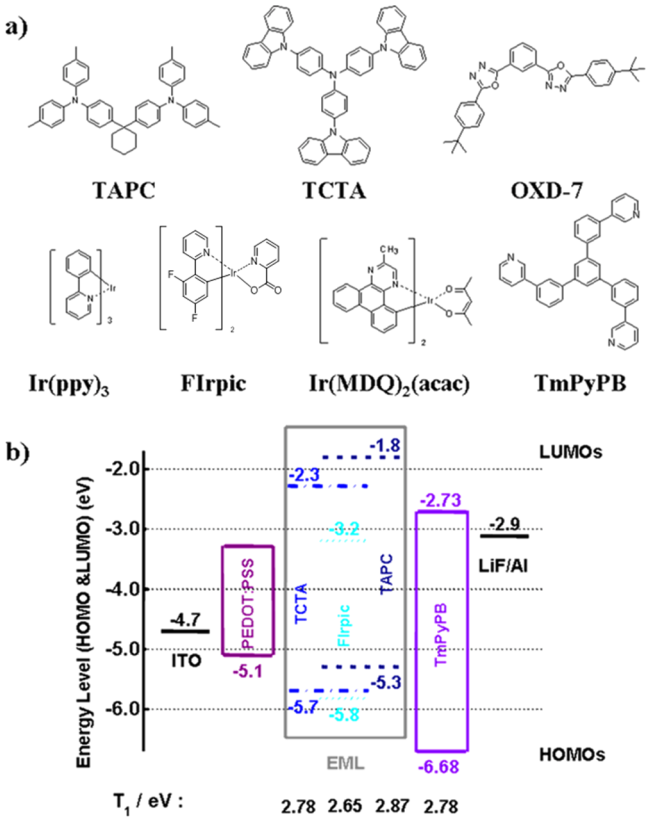

Figure 1. (a) Molecular structures and (b) energy diagrams of used materials in solution-processed OLEDs.[31−39].

Device Fabrication. The device structure and proposed energy diagram of the solution-processed OLEDs are shown in Figure 1b. All devices were fabricated on glass substrates precoated with a 180 nm thick layer of indium tin oxide (ITO) having a sheet resistance of 10 Ω per square. The ITO substrates were ultrasonically cleaned with detergent, deionized water, acetone and isopropanol, and then dried by blowing nitrogen over them. A layer of 40 nm thick PEDOT:PSS was spin-coated onto the precleaned ITO substrates, and then baked at 120 °C in a vacuum oven for 30 min to extract residual water. Afterward, the samples were moved into a glovebox under a nitrogen-protected environment (oxygen and water contents less than 1 ppm), and the emissive layers (EMLs) were spin-coated on top of PEDOT:PSS from chlorobenzene and then annealed at 120 °C in a vacuum oven for 30 min to remove residual solvent; the thickness of EMLs is about 40 nm. Following that, the samples were transferred to a thermal evaporator chamber (pressure less than 5 × 10^{-4} Pa) connected to the glovebox without exposure to the atmosphere. 50 nm TmPyPB, 1 nm LiF, and 150 nm Al were deposited sequentially by thermal evaporation. The overlap between ITO and Al electrodes was 16 mm^2 as the active emissive area of the devices.

Measurements. The current−luminance−voltage characteristics were measured by a Keithley source measurement unit (Keithley 2400 and Keithley 2000) with a calibrated silicon photodiode. The EL spectra were measured by SpectraScan PR650 spectrophotometer. The film thickness were determined by Dektak 6 M Profiler (Veeco Metrology Inc.). For photovoltaic measurement, the photocurrent−voltage characteristics were recorded using a computer-controlled Keithley 236 source meter under a white light illumination with intensity of 100 mW/cm^2. The surface morphology of the films were investigated by atomic force microscopy (AFM, SPA 300HV with a

SPI 3800N Probe Station, Seiko Instruments Inc., Japan). All the measurements were carried out in ambient atmosphere.

RESULTS AND DISCUSSION

Solution-Processed Blue OLEDs Based on TCTA:TAPC Mixed-Host. TCTA is a widely used commercial host material for phosphorescent OLEDs due to its high first-triplet energy level (T_1). As shown in Figure 1b, the T_1 of TCTA (2.78 eV) is higher than that of FIrpic (2.65 eV), which indicates that TCTA can act as the host for FIrpic. Besides, it had been demonstrated that the formation of TCTA film by solution-process was feasible.[20,23,25] Thus, we chose TCTA as one of the host materials to fabricate solution-processed blue phosphorescent OLEDs. In the blue OLEDs, an attractive electron-transporting material of TmPyPB with high T_1 (2.78 eV) and deep highest occupied molecular orbital (HOMO) level (−6.68 eV) was used as the electron-transporting layer (ETL).[36] The high T_1 of TmPyPB can suppress energy transfer from FIrpic to the adjacent ETL and enable consumption of all the triplet excitons contributing to the emission, and the deep HOMO level can confine holes within the EMLs. More interestingly, TmPyPB is of high electron mobility in the range from 7.0×10^{-4} to 1.0×10^{-3} cm^2/V s at the electric field between 2.5×10^5 V/cm and 6.4×10^5 V/cm,[36] which is even higher than the hole mobility of pristine TCTA (3×10^{-4} cm^2/V s at 5.0×10^5 V/cm).[37−39] Recently, Lee et al. reported that the hole mobility of TCTA decreased by more than 2 orders of magnitude when doping with the phosphorescent materials of $Ir(ppy)_3$ and $Ir(piq)_3$, which was due to the effect of the hole traps formed by the dopants.[40] Here we found that the doping of FIrpic into TCTA also influenced the hole transport in the solution-processed films. Figure 2 shows the characteristics of current density in the hole-dominated devices of ITO/PEDOT:PSS(40 nm)/TCTA or FIrpic-doped TCTA(40 nm)/MoO_3(5 nm)/Al and the electron-dominated device Al/LiF(1 nm)/TmPyPB(50 nm)/LiF(1 nm)/Al.

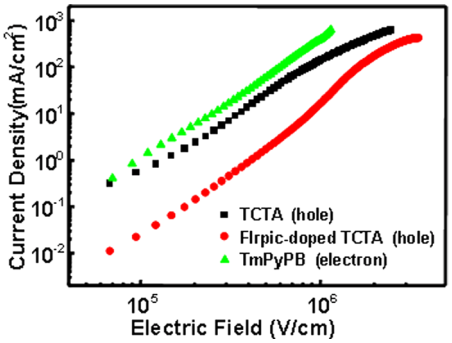

Figure 2. Current density characteristics in the hole-dominated devices ITO/PEDOT:PSS(40 nm)/TCTA or FIrpic-doped TCTA(40 nm)/MoO_3(5 nm)/Al and the electron-dominated device Al/LiF(1 nm)/TmPyPB(50 nm)/LiF(1 nm)/Al.

It is obvious that the hole current density decreases dramatically when FIrpic is introduced in the TCTA matrix. In FIrpic-doped TCTA films, the FIrpic molecules act as scatterers because the HOMO level of FIrpic is 0.1 eV lower-lying than that of TCTA as shown in Figure 1b. The decrease in the hole current density should be attributed to the hindering of hole transport by colliding in this scattering system.[25] The electron current density in the electron-dominated device of Al/LiF(1 nm)/TmPyPB-(50 nm)/LiF(1 nm)/Al was also shown in Figure 2. It can be found that the electron current density of the TmPyPB device is much higher than the hole current density of the FIrpic-doped TCTA device. This implies that electrons are the major carriers and holes are the minor carriers in the TCTA single-host blue OLED of ITO/PEDOT:PSS(40 nm)/TCTA:FIrpic(40 nm)/TmPyPB(50 nm)/LiF(1 nm)/Al. The imbalance of holes and electrons in the single-host device should lead to the triplet-polaron quenching, which will reduce the light emission. Hence, it may be useful to introduce another host into the EML to enhance hole injection and transport and thus to improve the device performance.

TAPC was usually used as the hole-transporting/electron-blocking layer because of its extreme high hole mobility (1×10^{-2} $cm^2/(V$ s) at 4.4×10^5 V/cm) and decent HOMO/LUMO levels.[34] And it was demonstrated that TAPC can also acted as the host material for FIrpic due to its high T_1 of 2.87 eV.[41] As shown in Figure 1b, the energy barrier between PEDOT:PSS and TAPC is only 0.2 eV, which is much lower than the energy barrier between PEDOT:PSS and TCTA (0.6 eV). So the hole injection could be improved by introducing TAPC into TCTA. On the other hand, the hole mobility of TAPC is about 2 orders of magnitude higher than that of TCTA, inferring that the doping of TAPC into TCTA would enhance the hole transport. Thus, it is believed that doping TAPC into TCTA can improve the charge balance in the blue OLEDs.

To investigate the effect of TAPC-doping on the device performance, we fabricated the blue phosphorescent OLEDs of ITO/PEDOT:PSS(40 nm)/TCTA:TAPC:FIrpic(15%)(40 nm)/TmPyPB (50 nm)/LiF (1 nm)/Al. Figure 3 shows the characteristics of current density−voltage, luminance−voltage, current efficiency (CE)−luminance, and power efficiency (PE)−luminance in the solution-processed blue devices with different TAPC concentrations. It can be found in Figure 3a that the current density obviously increases when 25 and 50% TAPC are doped into TCTA, which could be attributed to the improvement in both hole injection and transport as discussed above, whereas the current density of the TAPC single-host device (i.e., 100% TAPC) is much lower than that of the TCTA single-host device (i.e., 0% TAPC). This could result from the morphology effect of the solution-processed small molecule films (which will be discussed later). Table 1 summarizes the performances of the solution-processed blue OLEDs based on the hosts of TCTA, TAPC and their mixtures. It can be seen that the performances of the devices based on the mixed-host of TCTA:TAPC are much better than those of the devices using pure TCTA and TAPC as the single-host. The turn-on voltage (V_{on}) (defined as the voltage at 1 cd/m^2) are 3.5 and 3.9 V in the single-host devices based on TCTA and TAPC, respectively, which decreases to 3.0 V in the mixed-host devices. Notably, the best overall performance is obtained in the mixed-host device with 25% TAPC, in which a peak CE of 32.0 cd/A (at 156 cd/m^2) and a peak PE of 25.9 lm/W (at 38 cd/m^2) are achieved. Even at the luminance of 1000 cd/m^2, the CE and PE still reach 29.6 cd/A and 19.1 lm/W, respectively, and the driving voltage is as low as 4.9 V. The achieved PE value was one of the best efficiencies that have been reported for solution-processed blue phosphorescent OLEDs based on FIrpic.[7,25,42−46]

Figure 4 shows the electroluminescence (EL) spectra of the four solution-processed blue OLEDs at the luminance of 1000 cd/m^2. All of the devices only exhibit a FIrpic emission that is centered at 472 nm with vibrational peaks at long wavelengths, which indicates that the energy transfer from the single- and mixed-hosts to FIrpic is efficient. But the EL intensity at the vibrational peak slightly decreases with the concentration of TAPC. This could originate from the variation

dx.doi.org/10.1021/am301703a | ACS Appl. Mater. Interfaces 2012, 4, 6579−6586

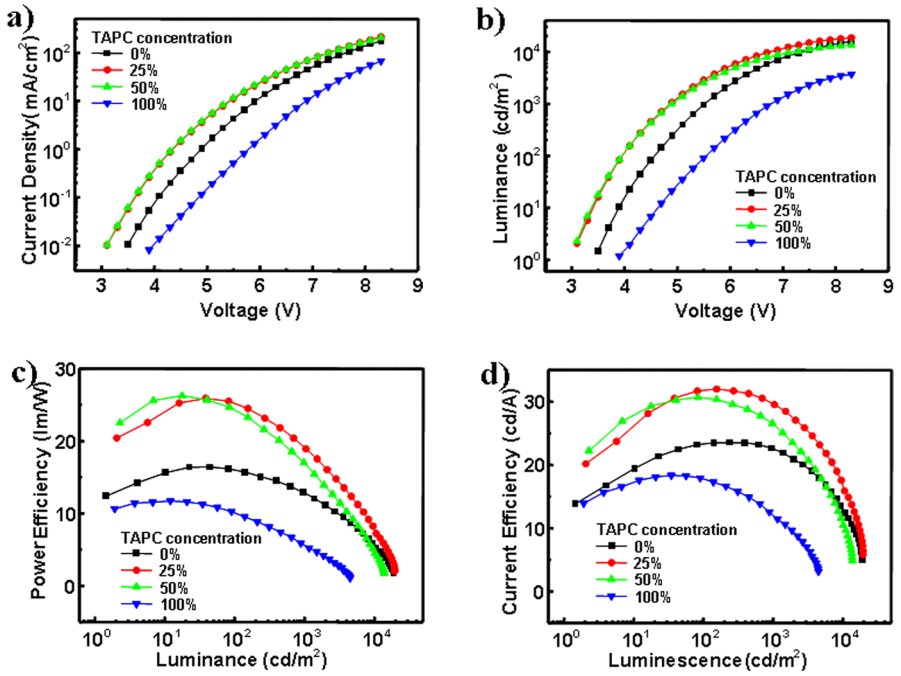

Figure 3. Comparison of the device characteristics in the solution-processed blue OLEDs based on the mixed-host of TCTA:TAPC with different TAPC concentrations: (a) current density−voltage, (b) luminance−voltage, (c) power efficiency−luminance, and (d) current efficiency−luminance.

Table 1. Device Performances of the Blue OLEDs Based on the Mixed Host of TCTA:TAPC with Different TAPC Concentrations

TAPC concentration (S)	V_{on} (V)	PE_{max} (lm/W)	CE_{max} (cd/A)	B_{max} (cd/m^2)	PE^a (lm/W)	CE^a (cd/A)	PE^b (lm/W)	CE^b (cd/A)
0	3.5	16.4	23.5	19 185	16.0	23.2	12.9	22.6
25	3.0	25.9	32.0	19 527	25.2	31.8	19.1	29.6
50	3.0	26.2	30.7	13 823	24.3	30.6	16.9	26.5
100	3.9	11.7	18.3	4534	10.1	17.8	5.6	12.1

^{a}The efficiencies at 100 cd/m^2. ^{b}The efficiencies at 1000 cd/m^2.

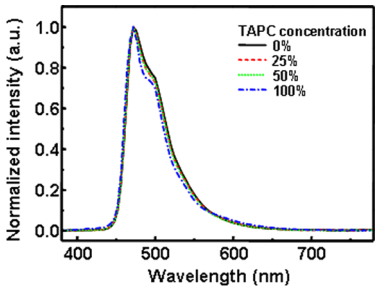

Figure 4. EL spectra of the solution-processed blue OLEDs with deferent TAPC concentrations at 1000 cd/m^2.

of optical lengths in the solution-processed EMLs because the density of the EMLs could be slightly different in the four devices. The Commission Internationale de l'Eclairage (CIE) coordinate in the TCTA and TAPC single-host devices are calculated to be (0.16, 0.34) and (0.16, 0.30), respectively. And the CIE in the TCTA:TAPC mixed-host devices are (0.16, 0.32).

Effect of TAPC on Hole Injection and Transport. The achieved low driving voltage and high efficiency in the mixed-host OLEDs should originate from the improvement of hole injection and transport by introducing TAPC in the EMLs. To verify the effect of TAPC-doping on the hole injection, we carried out photovoltaic measurements to determine the open circuit voltage (V_{oc}) in the TCTA:TAPC mixed-host blue OLEDs. As the cathode and ETL are identical in these devices, the V_{oc} is only influenced by the contact between the EMLs and PEDOT:PSS, which can reflect the capability of hole injection from ITO/PEDOT:PSS to the EMLs. The typical photovoltaic characteristics of the blue devices with varying TAPC concentrations in the EMLs are shown in Figure 5. In the

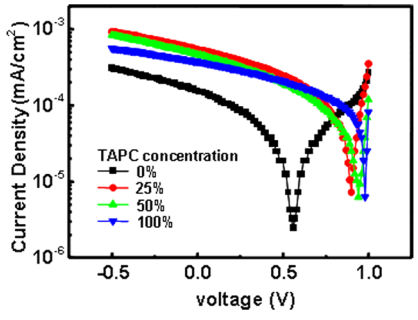

Figure 5. Photovoltaic characteristics of the solution-processed blue devices with different TAPC concentrations in the EMLs.

TCTA single-host device, the V_{oc} is only 0.56 V. When doping 25 and 50% TAPC in the EMLs, the V_{oc} increase to 0.90 and 0.94 V, respectively, which are very close to that of 0.98 V in the TAPC single-host device. The photovoltaic experiment

clearly demonstrates that the barrier for hole injection is reduced by incorporating TAPC into TCTA in the solution-processed blue OLEDs.

To get insight into the influence of TAPC-doping on the hole transport, we fabricated the hole-dominated devices with the structure of ITO/PEDOT:PSS(40 nm)/TCTA:TAPC:FIrpic(40 nm)/MoO_3(5 nm)/Al. Here, Al/MoO_3 is used as the anode to avoid the effect of hole injection because the HOMO of MoO_3 (−6.8 eV) is much deeper than those of TCTA, TAPC and FIrpic, resulting in unobstructed hole injection from the electrode to the EMLs.[47] Figure 6 shows the

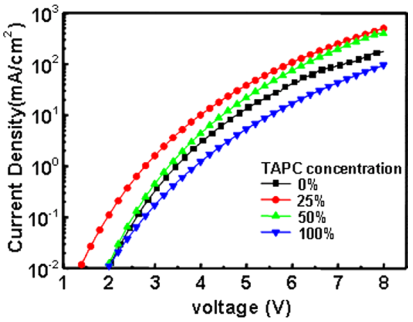

Figure 6. Current density−voltage characteristics of the hole-dominated devices ITO/PEDOT:PSS(40 nm)/TCTA:TAPC:FIrpic-(40 nm)/MoO_3(5 nm)/Al with different TAPC concentrations.

current density−voltage characteristics of the hole-dominated devices with varying TAPC concentration. The hole current density increases when incorporating TAPC into TCTA, but the current density in the device with 50% TAPC is lower than that of the device with 25% TAPC, which indicates that the introduction of an appropriate amount of TAPC can indeed improve the hole transport. It should be pointed out that the hole-dominated device with pure TAPC exhibits the lowest hole current density among the four hole-dominated devices, which is in accordance with the current density characteristics in the OLED based on TAPC single-host as shown in Figure 3a. To clarify this issue, the morphologies of the solution-processed small molecule films were investigated. Generally, the morphologies of solution-processed EMLs can significantly affect the charge transport property, which is directly related to the device performances.[11,32] Figure 7 shows the AFM images of the films of TCTA:TAPC:FIrpic spin-coated on the top of ITO/PSS:PEDOT with different TAPC concentrations. The root-mean-square (RMS) surface roughness of the solution-processed films with 0, 25, 50, and 100% TAPC are 0.39, 0.46, 0.47, and 0.77 nm, respectively. This demonstrates that the quality of the spin-coated TAPC film is poorer than that of the TCTA film, and the RMS surface roughness increases with the concentration of TAPC. Despite this, the roughness merely enhances 0.07 and 0.08 nm when incorporating 25 and 50% TAPC into TCTA, respectively, and neither aggregation nor phase separation is observed in the mixed-host EMLs. In contrast, obvious aggregation and defects appear in the TAPC single-host film, which should lead to inhibition of the hole transport and result in the worse device performance (see Figure 3 and Table 1).

Solution-Processed Blue OLEDs Based on TCTA:OXD-7 Mixed Host. In addition to enhancing charge injection and transport, another useful strategy for high efficiency OLEDs is to broaden recombination zone in EMLs.[48,49] For this purpose, bipolar materials containing both electron donor and acceptor moieties, or mixture system combining hole- and electron-transporting materials were proposed to act as host in phosphorescent OLEDs. Mixed-host could be advantageous over bipolar single-host because it is easy to control charge balance by simply blending without complicated synthesis. The electron-transporting OXD-7 was commonly utilized to blend with hole-transporting hosts for solution-processed blue phosphorescent OLEDs due to its good solution-processability and high T_1 (2.7 eV).[6,10,11,50,51] In this study, the blue OLEDs based on the TCTA:OXD-7 mixed-host were fabricated to compare with the devices based on the TCTA:TAPC mixed-host. The effect of OXD-7 concentration on the device performance was investigated. Figure 8 shows the efficiency characteristics in the solution-processed blue devices of ITO/PEDOT:PSS(40 nm)/TCTA:OXD-7:FIrpic(15%)(40 nm)/TmPyPB(50 nm)/LiF(1 nm)/Al with different OXD-7 concentrations. Table 2 summarizes their performance parameters. Although the V_{on} can be decreased in the TCTA:OXD-7 mixed-host devices, unfortunately, the efficiencies drop sharply when increasing the concentration of OXD-7 from 10% to 50%. This indicates that the introduction of OXD-7 into the EMLs is detrimental to the device performance in these solution-processed OLEDs. The lowered efficiency could be originated from the quenching of triplet excitons by PEDOT:PSS. As OXD-7 is incorporated into the mixed-hosts, the accumulated electrons at the EML/TmPyPB interface can move deeper into the EMLs, thus the recombination zone was broadened closer to the side of PEDOT:PSS. Because the diffusion length of triplet excitons is relatively long (can be over 10 nm) and the thickness of the solution-processed EMLs is only 40 nm, thus the formed triplet excitons can easily diffuse to the PEDOT:PSS/EML interface, where the excitons were quenched by PEDOT:PSS. Generally, a blocking layer inserted between PEDOT:PSS and EML was proposed to confine the exciton diffusion.[23,26] In addition, thickening EML was also used to reduce the quenching of excitons by PEDOT:PSS.[52] However, adding blocking layer and increasing EML thickness will increase the driving voltage and result in low power efficiency.[23,53] On the contrary, the use of TCTA:TAPC as the mixed-host can be free from these problems, because the improvement of hole injection and transport by TAPC can make the recombination zone closer to the EML/TmPyPB interface and thus effectively suppress the

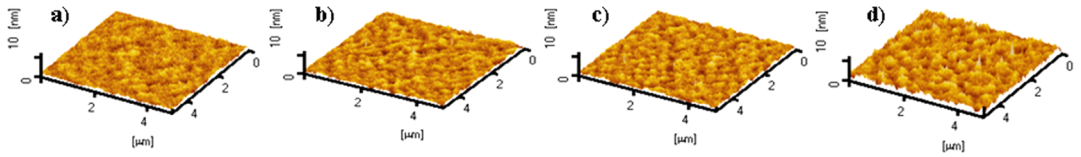

Figure 7. AFM images of the solution-processed small molecule films of TCTA:TAPC:FIrpic with different TAPC concentrations: (a) 0, (b) 25, (c) 50, and (d) 100%.

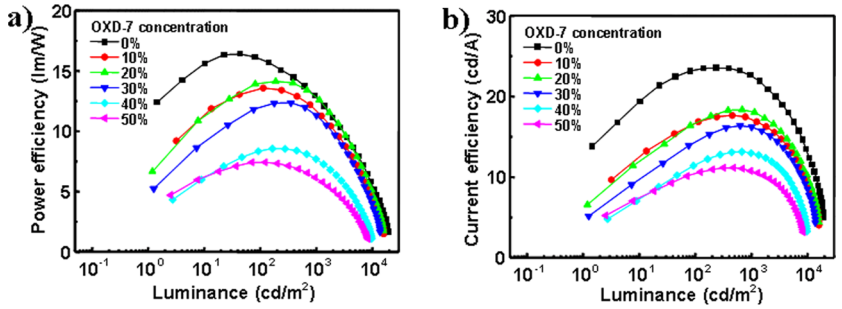

Figure 8. (a) Power efficiency and (b) current efficiency in the solution-processed blue OLEDs based on the mixed-host of TCTA:OXD-7 with different OXD-7 concentrations.

Table 2. Device Performances of the Blue OLEDs Based on the Mixed Host of TCTA:OXD-7 with Different OXD-7 Concentration

OXD-7 concentration (%)	V_{on} (V)	PE_{max} (lm/W)	CE_{max} (cd/A)	B_{max} (cd/m^2)	PE^a (lm/W)	CE^a (cd/A)	PE^b (lm/W)	CE^b (cd/A)
0	3.5	16.4	23.5	19 185	16.0	23.2	12.9	22.6
10	3.3	13.6	17.7	16 051	13.5	16.7	11.7	17.1
20	3.1	14.4	18.3	15 976	14.0	16.7	12.8	18.1
30	3.1	12.4	16.4	13 940	12.0	14.4	11.3	16.2
40	3.3	8.6	13.1	9369	8.4	11.5	7.7	13.0
50	3.5	7.4	11.2	8412	7.4	10.5	6.1	10.8

^{a}The efficiencies at 100 cd/m^2, ^{b}The efficiencies at 1000 cd/m^2

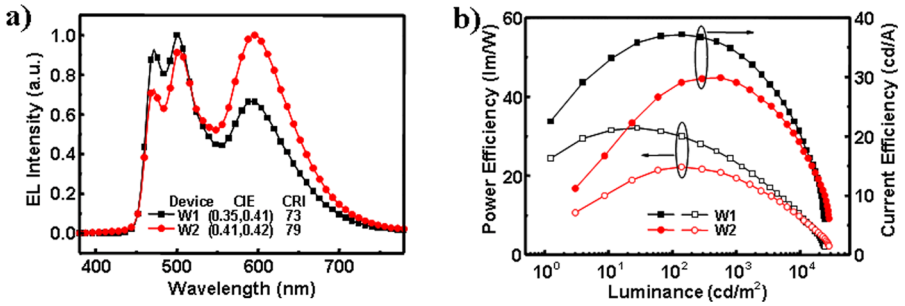

Figure 9. (a) EL spectra and (b) efficiencies of the solution-processed white OLEDs based on the mixed host of TCTA:TAPC.

exciton quenching at PEDOT:PSS/EML interface. So the low driving voltage and high power efficiency can be achieved in the TCTA:TAPC mixed-host devices.

Solution-Processed White OLEDs Based on TCTA:TAPC Mixed Host. Encouraged by the impressive results obtained from the solution-processed blue phosphorescent OLEDs based on the TCTA:TAPC mixed host, we fabricated white OLEDs with single emission layer by doping FIrpic, $Ir(ppy)_3$, and $Ir(MDQ)_2(acac)$ as the blue, green, and red emitters, respectively. Figure 9 shows the EL spectra (at 1000 cd/m^2) and efficiencies obtained from the two white OLEDs with the structure ITO/PEDOT:PSS(40 nm)/mixed-host:FIrpic:$Ir(ppy)_3$:$Ir(MDQ)_2(acac)$(40 nm)/TmPyPB (50 nm)/LiF (1 nm)/Al, where the mixed host is TCTA:TAPC with 25% TAPC. The concentration of FIrpic keeps at 15%, and the concentrations of $Ir(ppy)_3$ and $Ir(MDQ)_2(acac)$ are 0.5 and 0.3%, respectively, in the white device W1, and their corresponding concentrations are 1 and 0.6% in the device W2. As shown in Figure 9a, three separated peaks at 472, 504, and 596 nm are observed, which are corresponding to the emission from FIrpic, $Ir(ppy)_3$ and $Ir(MDQ)_2(acac)$, respectively, and their intensities are strongly dependent on the doping concentrations. W1 exhibits CIE of (0.35, 0.41) and color rendering index (CRI) of 73 at 1000 cd/m^2, whereas W2 gives CIE of (0.41, 0.42) and CRI of 79. It can be seen from Figure 9b that the efficiencies of W1 are higher than those of W2. A maximum CE of 37.1 cd/A and a maximum PE of 32.1 lm/W are obtained in the white device W1. Even at the luminance of 1000 cd/m^2, the CE and LE still reach 34.2 cd/A and 23.3 lm/W, respectively, and the driving voltage is as low as 4.6 V. In the device W2, the maximum CE and PE are 29.8 cd/A and 22.3 lm/W, respectively, which roll off to 29.0 cd/A and 19.4 lm/W at 1000 cd/m^2 (the driving voltage is 4.7 V). The obtained power efficiencies in the solution-processed small molecule OLEDs are comparable to those reported from vacuum-evaporation deposited white OLEDs.[54,55] It should be worth mentioning that the solution-process approach is more convenient than the vacuum-evaporation to fabricate the multicomponent EMLs, because it can easily realize the desired compositions of the EMLs by weighting, instead of the complicated coevaporation. This should be helpful for the fabrication of low-cost and high-efficiency white OLEDs for lighting applications.

CONCLUSION

This study demonstrates that some commercial small molecule materials can be used as solution-processed mixed-hosts to realize high-performance phosphorescent OLEDs. By incorporating

TAPC with high-lying HOMO and high hole mobility into TCTA, low-driving-voltage and high-efficiency blue and white phosphorescent OLEDs were achieved because of the improvement of hole injection and transport as well as the suppression of triplet exciton quenching at PEDOT:PSS/EML interface. A mixed-host blue OLED with the maximum PE of 25.9 lm/W was fabricated. And a maximum PE efficiency of 32.1 lm/W was achieved in a single-emissive-layer white OLED with three primary colors. Even at illumination-relevant luminance of 1000 cd/m^2, the PE still reached 23.3 lm/W and the driving voltage was only 4.6 V. Our study provides a good approach to develop low-cost and high-efficiency OLEDs for displays and lighting.

AUTHOR INFORMATION

Corresponding Author

*Tel.: +86 431 85262807/2357. Fax: +86 431 85262873. E-mail: jschen@ciac.jl.cn (J.S.C.); mdg1014@ciac.jl.cn (D.G.M.).

Notes

The authors declare no competing financial interest.

ACKNOWLEDGMENTS

The manuscript was written through contributions of all authors. All authors have given approval to the final version of the manuscript. This work was supported by the National Natural Science Foundation of China (60906020, 21161160442, 61036007), the Science Fund for Creative Research Groups of NSFC (20921061), Ministry of Science and Technology of China (973 program No. 2009CB623604, 2009CB930603), and the Foundation of Jilin Research Council (20090127, 201105028).

REFERENCES

(1) Tang, C. W.; VanSlyke, S. A. *Appl. Phys. Lett.* **1987**, *51*, 913−915.
(2) Burroughes, J. H.; Bradley, D. D. C.; Brown, A. R.; Marks, R. N.; Mackay, K.; Friend, R. H.; Burns, P. L.; Holmes, A. B. *Nature* **1990**, *347*, 539−541.
(3) Kamtekar, K. T.; Monkman, A. P.; Bryce, M. R. *Adv. Mater.* **2010**, *22*, 572−582.
(4) D'Andrade, B. W.; Forrest, S. R. *Adv. Mater.* **2004**, *16*, 1585−1595.
(5) Misra, A.; Kumar, P.; Kamalasanan, M. N.; Chandra, S. *Semicond. Sci. Technol.* **2006**, *21*, R35−47.
(6) Wu, H. B.; Zhou, G. J.; Zou, J. H.; Ho, C. L.; Wong, W. Y.; Yang, W.; Peng, J. B.; Cao, Y. *Adv. Mater.* **2009**, *21*, 4181−4184.
(7) Yook, K. S.; Jang, S. E.; Jeon, S. O.; Lee, J. Y. *Adv. Mater.* **2010**, *22*, 4479−4483.
(8) Zhang, Y.; Huang, F.; Jen, A. K.-Y.; Chi, Y. *Appl. Phys. Lett.* **2008**, *92*, 063303.
(9) Shih, P. I.; Shu, C. F.; Tung, Y. L.; Chi, Y. *Appl. Phys. Lett.* **2006**, *88*, 251110.
(10) Mathai, M. K.; Choong, V. E.; Choulis, S. A.; Krummacher, B.; So, F. *Appl. Phys. Lett.* **2006**, *88*, 243512.
(11) Huang, F.; Shih, P. I.; Shu, C. F.; Chi, Y.; Jen, A. K. Y. *Adv. Mater.* **2009**, *21*, 361−365.
(12) Zacharias, P.; Gather, M. C.; Rojahn, M.; Nuyken, O.; Meerholz, K. *Angew. Chem., Int. Ed.* **2007**, *46*, 4338−4392.
(13) Wu, H. B.; Zou, J. H.; Liu, F.; Wang, L.; Mikhailovsky, A.; Bazan, G. C.; Yang, W.; Cao, Y. *Adv. Mater.* **2008**, *20*, 696−702.
(14) Yang, X. H.; Jaiser, F.; Klinger, S.; Neher, D. *Appl. Phys. Lett.* **2006**, *88*, 021107.
(15) Wang, Z. K.; Lou, Y. H.; Naka, S.; Okada, H. *ACS Appl. Mater. Interfaces* **2011**, *3*, 2496−2503.
(16) Hou, L. D.; Duan, L.; Qiao, J.; Zhang, D. Q.; Dong, G. F.; Wang, L. D.; Qiu, Y. *Org. Electron.* **2010**, *11*, 1344−1350.
(17) Ye, T. L.; Shao, S. Y.; Chen, J. S.; Wang, L. X.; Ma, D. G. *ACS Appl. Mater. Interfaces* **2011**, *3*, 410−416.
(18) Gong, S. L.; Fu, Q.; Wang, Q.; Yang, C. L.; Zhong, C.; Qin, J. G.; Ma, D. G. *Adv. Mater.* **2011**, *23*, 4956−4959.
(19) Huang, H.; Fu, Q.; Zhuang, S. Q.; Liu, Y. K.; Wang, L.; Chen, J. S.; Ma, D. G.; Yang, C. L. *J. Phys. Chem. C* **2011**, *115*, 4872−4878.
(20) Chen, J. S.; Shi, C. S.; Fu, Q.; Zhao, F. C.; Hu, Y.; Feng, Y. L.; Ma, D. G. *J. Mater. Chem.* **2012**, *22*, 5164−5170.
(21) Huang, H.; Fu, Q.; Zhuang, S. Q.; Mu, G. Y.; Wang, L.; Chen, J. S.; Ma, D. G.; Yang, C. L. *Org. Electron.* **2011**, *12*, 1716−1723.
(22) Ren, Z. J.; Sun, D. M.; Li, H. H.; Fu, Q.; Ma, D. G.; Zhang, J. M.; Yan, S. K. *Chem.—Eur. J.* **2012**, *18*, 4115−4123.
(23) Park, J. J.; Park, T. J.; Jeon, W. S.; Pode, R.; Jang, J.; Kwon, J. H.; Yu, E. S.; Chae, M. Y. *Org. Electron.* **2009**, *10*, 189−193.
(24) Ding, Z. C.; Xing, R. B.; Fu, Q.; Ma, D. G.; Han, Y. C. *Org. Electron.* **2011**, *12*, 703−709.
(25) Doh, Y. J.; Park, J. S.; Jeon, W. S.; Pode, R.; Kwon, J. H. *Org. Electron.* **2012**, *13*, 586−592.
(26) Zheng, Y.; Eom, S. H.; Chopra, N.; Lee, J.; So, F.; Xue, J. G. *Appl. Phys. Lett.* **2008**, *92*, 223301.
(27) Goushi, K.; Kwong, R.; Brown, J. J.; Sasabe, H.; Adachi, C. *J. Appl. Phys.* **2004**, *95*, 7798−7805.
(28) Pingree, L. S. C.; Scott, B. J.; Russell, M. T.; Marks, T. J.; Hersam, M. C. *Appl. Phys. Lett.* **2005**, *86*, 073509.
(29) Zhao, Y. B.; Chen, J. S.; Ma, D. G. *Appl. Phys. Lett.* **2011**, *99*, 163303.
(30) Zhao, Y. B.; Zhu, L. L.; Chen, J. S.; Ma, D. G. *Org. Electron.* **2012**, *13*, 1340−1348.
(31) Giebelera, C.; Antoniadis, H.; Bradley, D. D. C.; Shirota, Y. *Appl. Phys. Lett.* **1998**, *72*, 2448.
(32) Cai, M.; Xiao, T.; Hellerich, E.; Chen, Y.; Shinar, R.; Shinar, J. *Adv. Mater.* **2011**, *23*, 3590−3596.
(33) Kuwabara, Y.; Ogawa, H.; Inada, H.; Noma, N.; Shirota, Y. *Adv. Mater.* **1994**, *6*, 677−679.
(34) Borsenberger, P. M.; Pautmeier, L.; Richert, R.; Bässler, H. *J. Chem. Phys.* **1991**, *94*, 8276−8281.
(35) D'Andrade, B. W.; Brooks, J.; Adamovich, V.; Thompson, M. E.; Forrest, S. R. *Adv. Mater.* **2002**, *14*, 1032−1036.
(36) Su, S. J.; Chiba, T.; Takeda, T.; Kido, J. *Adv. Mater.* **2008**, *20*, 2125−2130.
(37) Kang, J. W.; Lee, S. H.; Park, H. D.; Jeong, W. I.; Yoo, K. M.; Park, Y. S.; Kim, J. J. *Appl. Phys. Lett.* **2007**, *90*, 223508.
(38) Qiao, X. F.; Chen, J. C.; Ma, D. G. *Chin. Phys. Lett.* **2010**, *27*, 088504.
(39) Juang, F. S.; Hong, L. A.; Wang, S. H.; Tsai, Y. S.; Gao, M. H.; Chi, Y.; Shieh, H. P.; Hsu, J. S. *Jpn. J. Appl. Phys.* **2011**, *50*, 04DK04.
(40) Noh, S.; Sumana, C. K.; Hong, Y.; Leeb, C. *J. Appl. Phys.* **2009**, *105*, 033709.
(41) Chopra, N.; Swensen, J. S.; Polikarpov, E.; Cosimbescu, L.; So, F.; Padmaperuma, A. B. *Appl. Phys. Lett.* **2010**, *97*, 033304.
(42) Earmme, T.; Ahmed, E.; Jenekhe, S. A. *Adv. Mater.* **2010**, *22*, 4744−4748.
(43) Ye, S. H.; Liu, Y. Q.; Chen, J. M.; Lu, K.; Wu, W. P.; Du, C. Y.; Liu, Y.; Wu, T.; Shuai, Z. G.; Yu, G. *Adv. Mater.* **2010**, *22*, 4167−4171.
(44) Lee, J. I.; Chu, H. Y.; Yang, Y. S.; Do, L. M.; Chung, S. M.; Park, S. H. K.; Hwang, C. S. *Jpn. J. Appl. Phys.* **2006**, *45*, 9231.
(45) An, D.; Zou, J. H.; Wu, H. B.; Peng, J. B.; Yang, W.; Cao, Y. *Org. Electron.* **2009**, *10*, 299−304.
(46) Yook, K. S.; Lee, J. Y. *Org. Electron.* **2011**, *12*, 291−294.
(47) Hoping, M.; Schildknecht, C.; Gargouri, H.; Riedl, T.; Tilgner, M.; Johannes, H. -H.; Kowalsky, W. *Appl. Phys. Lett.* **2008**, *92*, 213306.
(48) Choong, V. E.; Shi, S.; Curless, J.; Shieh, C. L.; Lee, H. C.; So, F.; Shena, J.; Yang, J. *Appl. Phys. Lett.* **1999**, *75*, 172−174.
(49) Chen, Y. H.; Chen, J. S.; Zhao, Y. B.; Ma, D. G. *Appl. Phys. Lett.* **2012**, *100*, 213301.
(50) Xu, Y. H.; Yang, R. Q.; Peng, J. B.; Mikhailovsky, A. A.; Cao, Y.; Nguyen, T. Q.; Bazan, G. C. *Adv. Mater.* **2009**, *21*, 584−588.
(51) Ye, T. L.; Zhu, M. R.; Chen, J. S.; Ma, D. G.; Yang, C. L.; Xie, W. F.; Liu, S. Y. *Org. Electron.* **2011**, *12*, 154−160.

(52) Yim, K. H.; Friend, R.; Kim, J. S. *J. Chem. Phys.* **2006**, *124*, 184706.
(53) Leea, J. H.; Wu, C. I.; Liu, S. W.; Huang, C. A.; Chang, Y. *Appl. Phys. Lett.* **2005**, *86*, 103506.
(54) Eom, S. H.; Zheng, Y.; Wrzesniewski, E.; Lee, J.; Chopra, N.; So, F.; Xue, J. G. *Appl. Phys. Lett.* **2009**, *94*, 153303.
(55) Wang, Q.; Ding, J. Q.; Ma, D. G.; Cheng, Y. X.; Wang, L. X.; Wang, F. S. *Adv. Mater.* **2009**, *21*, 2397−2401.